A circumsolar ring of asteroidal dust in resonant lock with the Earth

Stanley F. Dermott, Sumita Jayaraman, Y. L. Xu, B. Å. S. Gustafson & J. C. Liou

Department of Astronomy, PO Box 112055, University of Florida, Gainesville, Florida 32611-2055, USA

Numerical simulations of the orbital evolution of asteroidal dust particles show that the Earth is embedded in a circumsolar ring of asteroidal dust, and has a cloud of dust permanently in its wake. This could account for the asymmetry of the zodiacal cloud observed by the Infrared Astronomical Satellite (IRAS). The resonant trapping and subsequent release of dust particles by the ring may provide a mechanism by which carbonaceous material is transported from the asteroid belt to the Earth.

ALL the observations of the distant Universe by spacecraft that operate in the infrared are made through a tenuous cloud of dust known as the zodiacal cloud that envelops the inner Solar System. Small, micrometre-sized particles in this cloud are removed by drag forces (Poynting–Robertson light drag and solar wind drag, that cause the particles to spiral in towards the sun)[1] on timescales $\sim 10^4$ years but are, presumably, continuously replenished[2]. Some of these interplanetary dust particles are deposited in, and collected from, the Earth's upper atmosphere and constitute a major source of extraterrestrial material[3]. However, their origin, whether asteroidal or cometary, is a matter of dispute[2].

In 1983, it was discovered that the zodiacal cloud is not featureless. IRAS revealed circumsolar, near-ecliptic bands of dust[4] that orginate in the asteroid belt, but probably extend to inside the orbit of the Earth[5], and seem to be related to the prominent asteroid families[6,7], that is, to known collision products in the asteroid belt. Modelling shows that the particles in these dust bands contribute ~10% of the thermal flux emitted by the zodiacal cloud and that dust from the main belt (between 2.2 and 3.3 astronomical units, where 1 AU is the Earth–Sun distance) is probably the source of about one-third of the thermal flux[8]. Due to the stochastic nature of collisions in the asteroid belt and our lack of knowledge of the number of small, collisionally-evolved asteroids in the outer regions of the asteroid belt, the latter estimate may be uncertain by a factor of two or more[9]. But we now know that the asteroid belt is certainly a significant source of zodiacal dust.

Gold[10], in a prescient paper, pointed out that small particles in the Solar System that spiral in towards the Sun (because of Poynting–Robertson light drag) may become trapped in resonances with the planets, with the result that the zodiacal cloud may have a banded appearance when viewed from outside the central plane. Resonances occur at those heliocentric distances for which the ratio of the orbital periods of the particles and the planets are ratios of small integers. In recent years, orbital evolution and resonant trapping of dust grains have been discussed by numerous authors with regard to planetary accretion[11–15] and the structure of the disk around β Pictoris[16–18]. From their numerical investigations of the orbital evolution of small dust grains, Jackson and Zook[19] made the specific suggestion that the Earth may be embedded in a ring of asteroidal particles in resonant lock with the planet.

The IRAS spacecraft has given us our highest resolution data on the structure of the zodiacal cloud. Dermott *et al.*[20] analysed these data and pointed out a marked but peculiar asymmetry, namely that the peak brightness of the zodiacal cloud in the trailing direction (that is, opposite to the Earth's orbital motion—see Fig. 1) is consistently greater than that in the leading direction. This finding was confirmed by Reach[21] who concluded, without detailed argument that either (1) there is a calibration inconsistency (in the gain) between the leading and trailing IRAS scans related to a radiation-induced responsivity enhancement produced by passage of the detectors through the South Atlantic Anomaly, or (2) there is an enhancement in dust density that follows the Earth around the Sun and that this could be related to the resonant trapping described by Jackson and Zook[19] or could be due to gravitational focusing.

We do not argue here that the IRAS data are devoid of calibration problems (hysteresis[21,22], for example, that is associated with passage through the South Atlantic Anomaly is clearly visible in the 25 μm data shown in Fig. 6*a*) or that these calibration problems are fully understood. The calibration scheme was based on a simple model of the zodiacal cloud and, as our knowledge of the observed and modelled structure of the zodiacal cloud grows, the IRAS model will inevitably prove to be inadequate. Our purpose is to show (1) that if, as we believe, asteroidal collisions are a significant source of zodiacal dust, then a trailing–leading asymmetry of the zodiacal cloud is to be expected, and (2) that the asymmetry observed by IRAS is quantitatively consistent with predictions based on our numerical

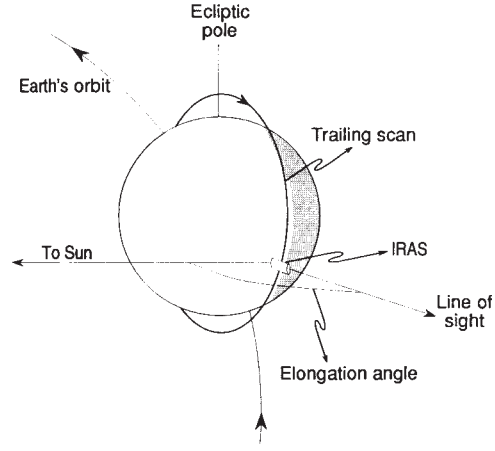

FIG. 1 Geometry of the IRAS observations. During each pole-to-pole scan of the sky, the elongation angle of the line of sight of the telescope was held constant.

investigations of the resonant trapping of asteroidal dust particles.

Dynamics of co-rotational resonance

The gravitational perturbations on the orbit of a dust particle in the Solar System can be separated into four distinct categories: short-period perturbations, resonant perturbations, secular (long-period) perturbations and direct scattering due to close encounters with the planets. The short-period perturbations are due to the gravitational attractions at planetary conjunction that repeat with the synodic period. The perturbations are resonant if the ratio of the periods of the bodies is a ratio of two small integers. Secular perturbations are due to the long-term averages of the forces between the planets and give rise to variations in the orbital eccentricities and inclinations. For particle diameters ranging from a few to a few hundred micrometres, non-gravitational forces are also important, particularly (1) light pressure and Poynting–Robertson light drag, and (2) solar wind drag due to the scattering of incident protons[1]. Drag forces remove angular momentum from the particles causing them to spiral in towards the Sun on timescales that increase directly with their diameters and are $\sim 5 \times 10^4$ years for spherical, 12-μm diameter, astronomical silicate particles[1].

Until the terrestrial planets are encountered, secular perturbations and drag forces largely determine the orbital evolution. The problem of describing orbital evolution due to secular perturbations in the presence of non-gravitational forces has been solved for asteroidal particles. Dermott *et al.*[5] have shown that the concepts of free and forced eccentricities and inclinations that arise from the solution of the secular perturbation equations without drag remain valid in the presence of drag. In particular, the proper inclinations remain constant whereas the proper eccentricities, e_0, decay with the semimajor axis, a, according to the two-body formulation of Wyatt and Whipple[23], that is,

$$\frac{de_0}{da} = \frac{5}{2}\frac{e_0}{a}\frac{(1-e_0^2)}{(2+3e_0^2)} \qquad (1)$$

and is independent of particle size. The forced inclinations and eccentricities can be calculated once the drag rates are specified[5].

Strong resonant interactions come into play as the particles spiral through the asteroid belt and encounter the Kirkwood gaps that correspond to mean motion resonances with Jupiter. Because the particles are moving away from Jupiter, that is, because their orbits and that of Jupiter are diverging, capture into resonance is unlikely and passage through these jovian resonances has little influence on the orbital elements[12,24]. But the same particles move on orbits that converge on those of the terrestrial planets and, although the terrestrial resonances are weaker than the jovian resonances, evolution on converging orbits allows capture into resonance[24]. We confirm this by direct numerical integration of the full equations of motion for 12-μm-diameter asteroidal particles using the RADAU fifteenth-order integrator program with variable time steps taken at Gauss–Radau spacings[25]. We consider spherical astronomical silicate[1] particles of density 2.7 g cm^{-3} for which the ratio of radiation pressure to gravitational force, β, is 0.037. The average force due to the solar wind is taken to be 30% of the Poynting–Robertson light drag force, varying on a 11-year cycle from 20% to 40% (ref. 1). The initial distributions of the proper inclinations and eccentricities are the same as those of the brighter asteroids in the main belt. Under these conditions, numerical integration of the orbits of 912 particles originating in the main belt shows that ~20% of these particles are trapped in first-order co-rotational resonances outside the Earth's orbit (Fig. 2).

If we retain only the leading term in the disturbing function of the particle, then the equation of motion of the resonant argument, ϕ, defined by

$$\phi = p\lambda - (p+1)\lambda' + \bar{\omega}' \qquad (2)$$

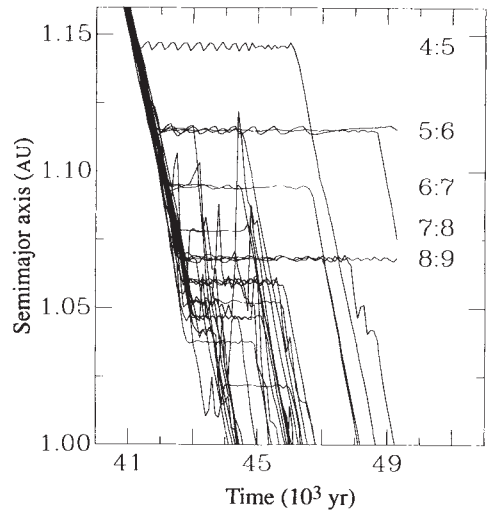

FIG. 2 Orbital evolution of 12-μm-diameter asteroidal dust particles of density 2.7 g cm^{-3} and $\beta = 0.037$, showing capture into (and escape from) p: $(p+1)$ resonances outside the orbit of the Earth (see text and equation (2) for definition of β and p). The orbits of 912 particles with initial elements identical to those of a bias-free set of main-belt asteroids were integrated numerically. This plot shows the orbital history of the 28 of the 114 particles originating in the inner part of the belt that were trapped in resonance with the Earth.

is that of a damped harmonic oscillator and the acceleration of ϕ, $\ddot{\phi}$, is given by

$$\ddot{\phi} = -(Gm/a')f(\alpha, \beta)e' \sin \phi - (p+1)\dot{n}_d' \qquad (3)$$

where p is an integer, λ is the mean longitude, $\bar{\omega}$ is the longitude of perihelion, Gm is the gravitational mass of the Earth, a is the semimajor axis, e the eccentricity, $\alpha = a/a'$, $f(\alpha, \beta)$ is a function of Laplace coefficients and β that increases markedly with increasing p, $\dot{n}_d'$ is the average rate of change of the mean motion n' due to the action of drag, unprimed quantities refer to the orbit of the Earth and primed quantities refer to the orbit of the dust particle[13].

The path of a particle librating in a 5:6 corotational resonance with the Earth is shown in Fig. 3. Without drag, the path would have mirror symmetry about the mean Earth–Sun line. But drag introduces a phase lag into the equation of motion, with the result that the path is asymmetric; as the particles pass through perihelion, they approach the Earth closer in the trailing direction (behind the Earth in its orbit) than in the leading direction.

Predicted ring structure

By setting the left-hand side of equation (3) to zero, we find that the phase lag is a maximum ($|\sin \phi| \approx 1$), when

$$|(Gm/a')f(\alpha, \beta)e'| \approx |(p+1)\dot{n}_d'| \qquad (4)$$

and the strength of the resonance is just sufficient to counteract the effect of drag on the particle's semimajor axis. While the particle is trapped in resonance, drag acts quickly to increase the particle's eccentricity e' and the strength of the resonance[24]. Paradoxically, this leads to resonance disruption on timescales $\lesssim 10^4$ years (Figs 2 and 4). This is caused by the onset of chaos due to resonance overlap[24] and, probably more importantly, direct particle scattering due to close encounters with the Earth[26–28], once drag has reduced the particle's perihelion to inside the Earth's orbit. The disruption timescales are smaller than, but comparable with, the collision lifetimes of the particles[2], and interparticle collisions will have to be considered in a more complete analysis of the ring's structure.

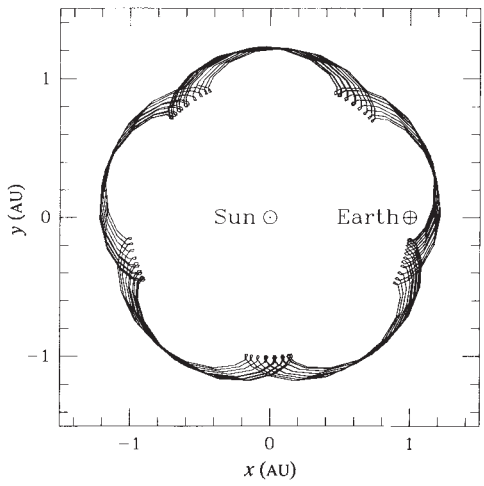

FIG. 3 The path of a 12-μm-diameter asteroidal dust particle trapped in a 5:6 resonance with the Earth is shown, not in an inertial frame, but in a frame centred on the Sun and co-rotating with the Earth's mean motion (the Earth is near-stationary in this frame). The motion of the particle is tracked over one complete libration period of the resonant argument. Particles of this size experience large drag forces, with the result that their paths are not symmetric about the Sun–Earth line.

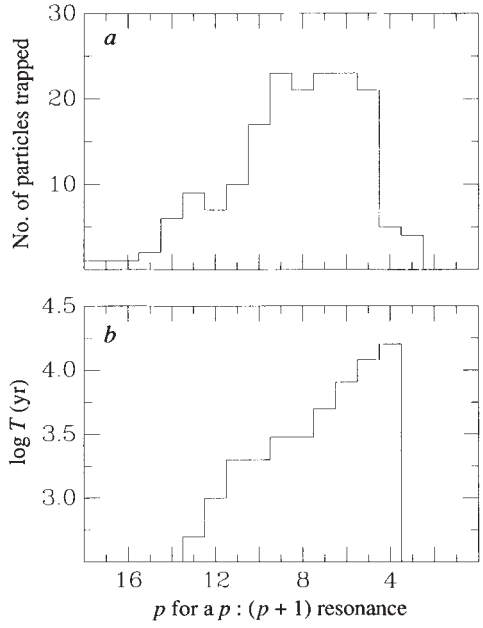

FIG. 4 *a*, The relative probability of capture into, and *b* the average trapping time T in, p: $(p+1)$ resonances outside the orbit of the Earth of 12-μm-diameter asteroidal dust particles. The orbits of 912 particles with initial elements identical to those of a bias-free set of main-belt asteroids were integrated numerically. The p values of the 169 particles that were trapped in resonance are shown in *a*, and their average trapping times in those resonances are shown in *b*.

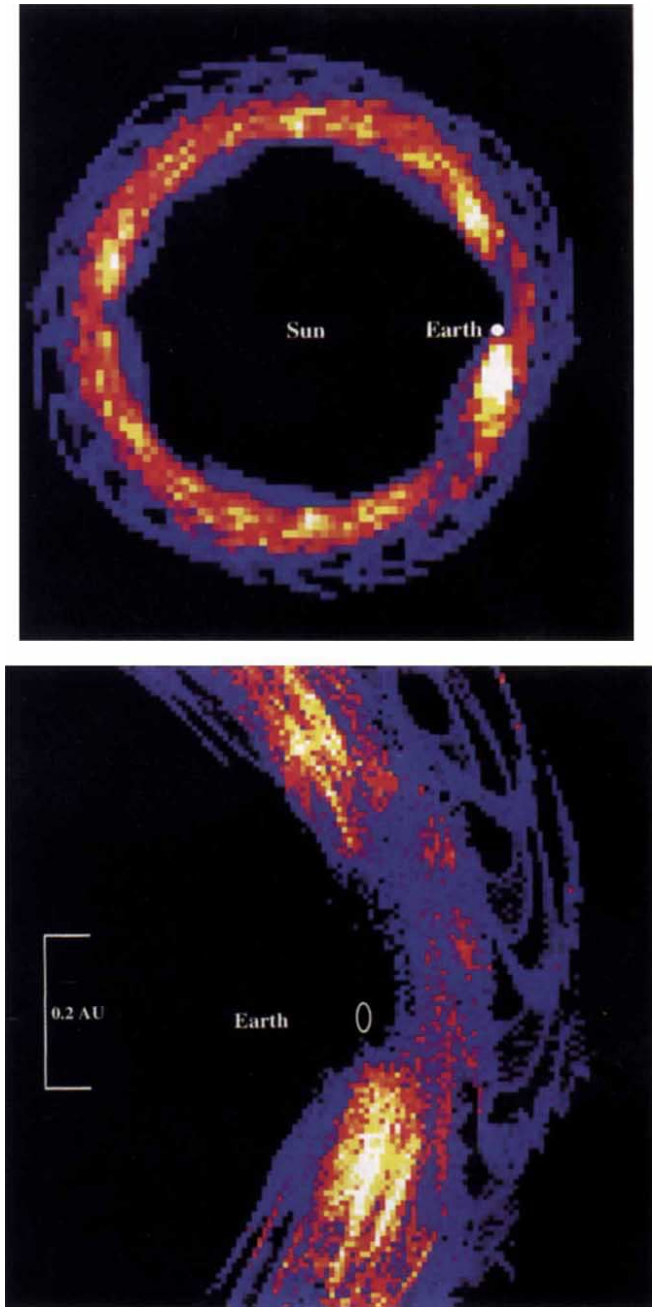

FIG. 5 Top, numerical simulation of the structure of a heliocentric ring of asteroidal dust particles in a frame centred on the Sun and co-rotating with the Earth. The cloud of particles that appears to trail the Earth in its orbit has a peak particle number density (colour-coded white) ~10% greater than that of the background zodiacal cloud. The resolution of the image is (0.04 × 0.04 AU). Bottom, higher-resolution image (0.01 × 0.01 AU) of the numerical simulation shown above. On this scale, the eccentricity of the Earth's orbit ($e = 0.0167$) is apparent and the Earth's path in the co-rotating frame is depicted by the small 2:1 ellipse: motion around this ellipse is clockwise. The Earth passes through perihelion in the first week of January, and is closest to the trailing part of the ring in the first week of October.

The structure of the ring produced by resonant trapping is estimated from our numerical integrations. We consider main-belt asteroidal particles, because the high orbital accentricities of both cometary particles and particles deriving from the disruption of near-Earth asteroids make resonant trapping highly improbable[19,29]. The size–frequency distribution of asteroidal particles is such that the effective area of dust, and hence the thermal flux from the ring observed in a given IRAS waveband, may be dominated by flux from the near-smallest particles in the distribution (that is, particles with radii $\gtrsim \Lambda/2\pi$—where Λ is the waveband of the detector—that are also large enough to satisfy the resonance strength criterion given by equation (4)). These particles also have the highest phase shifts, with the result that the dynamics of resonance is in the non-adiabatic regime[24] (for which analytic theory is only a guide) and reliable results must be obtained by numerical integration. The drag rates on very small particles can be too high to allow resonance trapping,

the critical size varying with the particle's eccentricity e' and the p value of the resonance[26]. To obtain a detailed description of the structure of the ring, the dynamics of a wide range of particle sizes need to be considered. The size–frequency distribution of asteroidal particles near the Earth is uncertain, especially if asteroidal particles are not the dominant source of the zodiacal cloud. We estimate that asteroidal particles of diameter 12 μm and density 2.7 g cm^{-3} are close to the critical size for trapping into the most significant resonances. We have also shown that the dynamics of particles of about this size can account for the observed plane of symmetry of the background zodiacal cloud[5]. Here we estimate the structure of the ring from the dynamics of these particles alone.

We consider that a particle is trapped if it remains in a given resonance for at least ~500 years, or more than one libration period. On integrating the orbits of 912 particles, we find that up to 20% of the particles are trapped in first-order resonances with p: $(p+1)$ ranging from 3:4 to 17:18 with occasionally even higher values of p. Figure 4*a* shows the relative probability of capture into the individual resonances. We determine the average trapping time for particles in these resonances empirically (Fig. 4*b*). The trapping times decrease sharply with increasing p as the locations of the resonances get closer to the Earth and the probability of close encounters increases. The overall distribution of particles in the ring at any given time is a convolution of the quantities given in Fig. 4*a* and *b* with the distributions of the positions of the particles in the various resonances, as tracked in the rotating reference frame, from the time of capture to the typical time of release.

Our final model is a simulated 'image' binned in pixels of 0.04 × 0.04 AU (Fig. 5). The 5:6 resonance shown in Fig. 3 has five lobes, with the Earth residing asymmetrically in one of those lobes. All other resonances have similar structures, only the number of lobes varies. The resultant image obtained by superposition of the various paths weighted according to the probability of capture and the trapping times shows that, in a rotating reference frame, the trapped particles form a near-uniform ring around the Sun that co-rotates in inertial space with the Earth.

The peripheral arc-like structures in the ring are artefacts caused by the limited number of single-size particles considered in the model. We consider, however, that the other noticeable features in Fig. 5 are real. First, the existence of a cavity in the ring at the location of the Earth (see also ref. 30). Figure 5 also shows that apart from an asymmetry in the mean position of the Earth in the ring's cavity, there is also a marked asymmetry in the longitudinal variation of the particle number density. The increase in resonance strength—and the corresponding decrease in phase shift with increasing p value—disperses the longitudes of the perihelia of the particle paths in the rotating frame in the leading direction, while concentrating the longitudes of the perihelia in the trailing direction. This results in a marked enhancement of particle number density behind the Earth in its orbit, as if the Earth had a trailing cloud of dust permanently in its wake.

Observed zodiacal cloud asymmetry

The observed trailing–leading asymmetry is most clearly revealed by exploiting the IRAS observing sequence. To obtain good all-sky coverage, the elongation angle used by IRAS was not held constant at 90°, but was shifted systematically from scan to scan over periods of a few weeks to ensure complete coverage of the sky. For the first two-thirds of the mission, the elongation angle, while being kept within about 10° of 90°, was incrementally increased from scan to scan for scans in the trailing direction, whereas for scans in the leading direction the elongation was incrementally decreased. These regularities allow us to increase the signal-to-noise ratio by using all the data obtained in a given period (of a few weeks) to obtain (1) the average brightness for an elongation angle of 90°, and (2) the Earth's ecliptic longitude when that elongation angle was measured.

A plot of the variation with elongation angle of the peak near-ecliptic brightness of the broad-scale zodiacal background observed by IRAS in three wavebands from 9 to 11 July 1983 is shown in Fig. 6*a* (Fourier methods are used to separate the smooth, large-scale zodiacal background from the signals associated with the narrower asteroidal dust bands[20]). We have obtained similar plots for all the other periods of the mission for which data were obtained that encompass an elongation angle of 90° and that are not overly contaminated by noise deriving from proximity to the Galactic plane. Variations of the average brightness for an elongation angle of 90° with the ecliptic longitude of the Earth in both the trailing and leading directions are shown in Fig. 6*b*.

There are three reasons why the peak brightness of the zodiacal cloud should vary with ecliptic longitude when viewed at a constant elongation angle[31]. These arise from the forced eccentricities of the dust particle orbits[20], from the inclination of the plane of symmetry of the cloud with respect to the ecliptic and from the Earth's orbital eccentricity. By modelling a cloud of asteroidal dust particles[31], we have shown (1) that the Earth's orbital eccentricity is the dominant effect and (2) that the peak

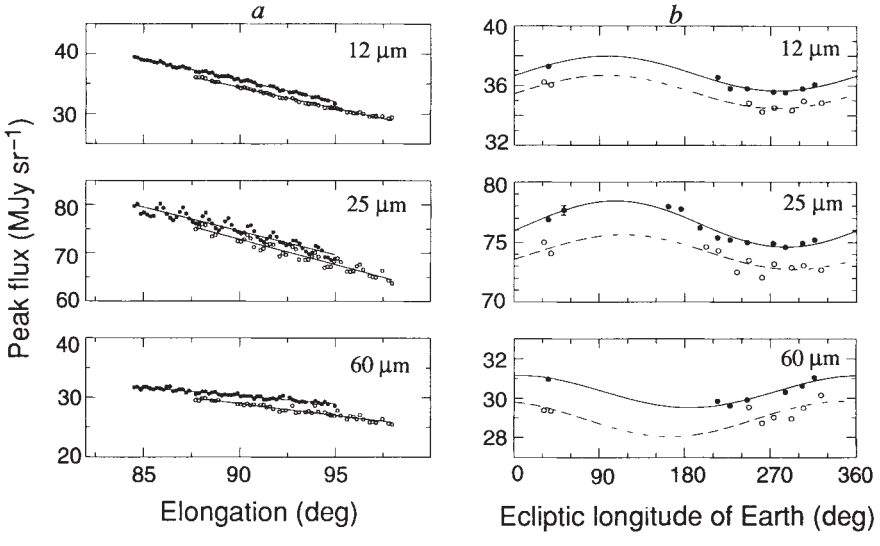

FIG. 6 *a*, (Left-hand column) variation of the peak (near-ecliptic) brightness of the large-scale background zodiacal cloud with elongation angle, in three separate wavebands. The data in the leading direction (that is, in the direction of the Earth's orbital motion) are from 9 to 17 July 1983 (open circles). The data in the trailing direction (that is, in the direction opposite to the Earth's orbital motion) are from 4 to 12 July 1983 (filled circles). The best-fit straight lines are used to determine the peak fluxes corresponding to an elongation angle of 90°. *b*, (right-hand column) variation with the Earth's ecliptic longitude (or time of the year) of the peak (near-ecliptic) brightness of the large-scale zodiacal cloud observed by IRAS in three separate wavebands at an elongation angle of 90° in the trailing direction (solid line and filled circles) and in the leading direction (broken line and open circles). In all cases except one, the magnitudes of the error bars of the points (derived from plots similar to those in *a*) are too small to show.

TABLE 1 Variation of the peak flux observed by IRAS

Waveband μm	Direction	Longitude of Earth for peak flux (degrees)	Mean flux (MJy sr^{-1})	Flux ratio (T/L)
12	T	98 ± 6	36.82 ± 0.13	1.035 ± 0.007
12	L	97 ± 13	35.59 ± 0.21	
25	T	106 ± 5	76.52 ± 0.16	1.031 ± 0.004
25	L	118 ± 17	74.19 ± 0.26	
60	T	5 ± 11	30.34 ± 0.13	1.045 ± 0.016
60	L	345 ± 26	29.03 ± 0.44	

These measurements were made at an elongation angle of 90° in the trailing (T) and leading (L) directions.

brightness in both the leading and trailing directions should occur when the Earth is close to perihelion, that is, at an ecliptic longitude of 102.3°. These variations are clearly observed in both the 12-μm and the 25-μm wavebands (Fig. 6*b* and Table 1). The weighted average of the ecliptic longitudes of the Earth associated with the peaks of the sine curves fitted to the 12-μm and 25-μm data is 103 ± 5°. The data in the 60-μm waveband are not consistent with those in the other wavebands. This could be due to a contribution of thermal flux from the Galaxy, but this needs to be verified. But ratios of fluxes are insensitive to calibration errors, and Fig. 6*b* shows that in all three wavebands, at all times of the year, observations in the trailing direction are brighter than those in the leading direction by 3 or 4% (the precise mean ratios for each waveband, that depend on fitting sine curves through the data, are given in Table 1).

We consider that the asymmetries of the Earth's resonant ring that arise from (1) the position of the Earth near the trailing edge of a cavity in the ring and (2) the cloud of asteroidal particles that trails the Earth in its orbit, act together to produce the observed trailing-to-leading flux ratios. If we assume that all the particles in the zodiacal cloud are asteroidal and of diameter 12 μm, then we calculate that the asymmetry between the trailing and leading flux due to the ring is as high as 12%. But recent calculations, using two new results (that the particles in the dust bands are asteroidal and constitute 10% of the cloud, and that the ratio of the thermal flux from the asteroidal families to that from the entire main-belt of asteroids is 1:3.4), lead us to estimate that about one-third of the zodiacal cloud is asteroidal in origin[8] (see also Reach[32]). Therefore, if only one-third of the cloud is made up of asteroidal particles (that is, particles of low orbital eccentricity) that can be trapped in the ring, the asymmetry in the flux will decrease from 12 to 4% which is comparable to the observed value. But the dust in the zodiacal cloud must have a size–frequency distribution and its effect has to be studied carefully. Because asteroidal particles in the cloud with diameters $\lesssim 5$ μm do not get trapped in the ring, they will tend to decrease the amount of asymmetry, whereas the larger particles in the cloud, although less in number, have higher probabilities of capture into resonances (because of their smaller drag rates) and will increase the flux from the ring. Using data from the Cosmic Background Explorer (COBE) satellite, we will obtain a more precise estimate of the trailing–leading asymmetry, not only at 25 μm but at a range of wavelengths which will enable us to develop a more sophisticated model of the ring that includes a range of particle sizes. Precise measurements of the ratio of trailing flux to leading flux will allow us to determine the contribution of asteroidal particles to the near-Earth region of the zodiacal cloud, and may place constraints on their size–frequency distribution.

From the model shown in Fig. 5, we can predict two effects due to the Earth's epicycle: (1) a yearly variation in the flux ratio, and (2) a higher probability of interplanetary dust particles encountering the Earth at certain times of the year. Both of these effects will be a maximum in the second half of the year (around September/October) when the Earth is closest to the trailing cloud. This annual variation of the asymmetry will provide further constraints on the number distribution of asteroidal particles in the zodiacal cloud, and can be determined from the COBE data which has more accurate flux calibration as well as extensive coverage in both elongation angle and wavelength. The release of particles from the ring due to close encounters may make the ring act as a funnel which directs particles in near-circular orbits into the Earth's upper atmosphere. This may prove to be a mechanism for the delivery of carbonaceous material from the asteroid belt to the Earth. Further studies are needed to determine the fraction of particles actually colliding with the Earth.

This mechanism of ring formation is not exclusive to the Earth and can be extended to other terrestrial planets. Both Mars and Venus will favour the capture of larger particles which have lower drag-rates. This is because even though the particles have lower drag rates near Mars, the martian mass is only 10% of that of the Earth's and the martian resonances are correspondingly weaker. In the case of Venus, the particles are moving with a higher drag-rate. Mercury is unable to capture significant numbers of particles because of its very low mass and the higher drag-rates of particles close to the Sun.

Extending this phenomenon outside our Solar System, the discovery of large disks around stars like β Pictoris (by IRAS) and Fomalhaut[33] suggests that resonance effects may play an important role in the detection of other planetary systems. Resonances can give rise to features like arcs and gaps in the disk of dust surrounding the star, indicating the presence of a planet which may otherwise be undetectable[15–18]. □

Received 8 April; accepted 25 May 1994.

1. Gustafson, B. Å. S. *A. Rev. Earth & planet. Sci.* **22,** 553–595 (1994).
2. Grün, E., Zook, H. A., Fechtig, H. & Giese, R. H. *Icarus* **62,** 244–272 (1985).
3. Bradley, J. P., Sandford, S. A. & Walker, R. M. in *Meteorites and the Early Solar System* (eds Kerridge, J. F. & Matthews M. S.) 861–895 (Univ. Arizona, Tucson, 1988).
4. Low, F. J. *et al. Astrophys. J.* **278,** L19–L22 (1984).
5. Dermott, S. F. *et al.* in *Chaos, Resonance, and Collective Dynamical Phenomena in the Solar System* (ed. Ferraz-Mello, S) 333–347 (Kluwer, Dordrecht, 1992).
6. Dermott, S. F., Nicholson, P. D., Burns, J. A. & Houck, J. R. *Nature* **312,** 505–509 (1984).
7. Sykes, M. V. *Icarus* **84,** 267–289 (1990).
8. Dermott, S. F. *et al.* in *Asteroids, Comets, Meteors 1993* (eds Milani, A. & Di Martino, M.) (Kluwer, Dordrecht, in the press).
9. Durda, D. D. thesis, Univ. Florida (1993).
10. Gold, T. *Icarus* **25,** 489–491 (1975).
11. Greenberg, R. *Icarus* **33,** 62–73 (1978).
12. Gonczi, R., Froeschlé, Ch. & Froeschlé, C. *Icarus* **51,** 633–654 (1982).
13. Weidenschilling, D. & Davis, D. *Icarus* **62,** 16–29 (1985).
14. Patterson, C. W. *Icarus* **70,** 319–333 (1987).
15. Sicardy, B., Beaugé, C., Ferraz-Mello, S., Lazzaro, D. & Roques, F. *Celest. Mech. dyn. Astr.* **57,** 373–390 (1993).
16. Scholl, H., Roques, F. & Sicardy, B. *Celest. Mech. dyn. Astr.* **56,** 381–393 (1993).
17. Roques, F., Scholl, H., Sicardy, B. & Smith, B. *Icarus* **108,** 37–58 (1994).
18. Lazzaro, D., Sicardy, B., Roques, F. & Greenberg, R. *Icarus* **108,** 59–80 (1994).
19. Jackson, A. A. & Zook, H. A. *Nature* **337,** 629–631 (1989).
20. Dermott, S. F., Nicholson, P. D., Kim, Y., Wolven, B. & Tedesco, E. F. in *Comets to Cosmology* (ed. Lawrence, A.) 3–18 (Springer, Berlin, 1988).
21. Reach, W. T. *Astrophys. J.* **369,** 529–543 (1991).
22. Deul, E. R. & Walker, H. J. *Astr. Astrophys. Suppl. Ser.* **81,** 207–214 (1989).
23. Wyatt, S. P. & Whipple, F. L. *Astrophys. J.* **111,** 134–141 (1950).
24. Dermott, S. F., Malhotra, R. & Murray, C. D. *Icarus* **76,** 295–334 (1988).
25. Everhart, E. in *Dynamics of Comets* (eds Carusi, A. & Valsecchi, G. B.) 185–202 (Reidel, Dordrecht, 1985).
26. Weidenschilling, S. & Jackson, A. A. *Icarus* **104,** 244–254 (1993).
27. Jackson, A. A. & Zook, H. A. *Icarus* **97,** 70–84 (1992).
28. Marzari, F. & Vanzani, V. *Astr. Astrophys.* **283,** 275–286 (1994).
29. Liou, J. C. thesis, Univ. Florida (1993).
30. Jackson, A. A. & Zook, H. A. *Lunar planet. Sci.* **XXIII,** 595–596 (1992).
31. Xu, Y. L. *et al.* in *The Ceremony of the 70th Anniversary of the Chinese Astronomical Society* (Chinese Acad. Sci., Beijing, in the press).
32. Reach, W. T. in *Origin and Evolution of Interplanetary Dust* (eds Levasseur, A. C. & Hasegawa, H.) 211–214 (Kluwer, Dordrecht, 1991).
33. Stern, S. A., Weintraub, D. A. & Festou, M. C. *Nature* **368,** 312–314 (1994).

ACKNOWLEDGEMENTS. We thank J. A. Burns and W. T. Reach for comments, and the Department of Computer Sciences at the University of Florida for use of the KSR1 Parallel Supercomputer. This work was supported by NASA, the University of Florida, the IBM Corporation and the Geophysics Directorate of the US Air Force Phillips Laboratory.